RSC Advances

Cite this: *RSC Advances*, 2011, **1**, 1207–1210

www.rsc.org/advances

COMMUNICATION

Monodisperse CeO_2/CdS heterostructured spheres: one-pot synthesis and enhanced photocatalytic hydrogen activity†

Xi-Hong Lu,[a] Shi-Lei Xie,[a] Teng Zhai,[a] Yu-Feng Zhao,[a] Peng Zhang,[a] Yue-Li Zhang[b] and Ye-Xiang Tong*[a]

Received 1st June 2011, Accepted 6th September 2011
DOI: 10.1039/c1ra00252j

Well-dispersed and highly-crystalline CeO_2/CdS heterostructured spheres with diameters of about 500 nm were directly grown on fluorine-doped tin oxide (FTO) substrates *via* electrodeposition from aqueous solution. These CeO_2/CdS heterostructured spheres exhibit an enhanced photocatalytic performance in hydrogen production.

Photocatalytic hydrogen evolution using semiconductors has been of significant interest as a promising means for the large-scale production of hydrogen since it utilizes renewable resources without yielding carbon dioxide directly.[1–2] Many semiconducting photocatalysts have been developed to produce hydrogen from water under light irradiation, and great advances have been made.[3–4] However, most of them are transition metal oxides with wide band gaps that are capable of capturing only ultraviolet irradiation (about 4% of solar energy). As a result, increasing attention has been paid to developing visible-light-driven photocatalysts for the more efficient utilization of solar energy.[5] Sulfides are attractive visible-light-driven photocatalysts because they have narrow band gaps and conduction bands at relatively negative potentials. Among them, CdS is one of the classical II–VI group semiconductors with a direct band gap of 2.4 eV, which has been extensively studied in photocatalytic hydrogen production due to its ability in harvesting visible light and suitable conduction band potential.[6–8] However, the utility of CdS as a photocatalyst has been limited due to its anodic decomposition (photocorrosion) where CdS itself is oxidized by photogenerated holes.[9]

In recent years, considerable efforts have been made to enhance the photocatalytic activity of CdS, and several strategies have been proposed.[10–12] Among them, combining CdS with metal oxides has proven to be one of the most effective strategies for the enhancement of photocatalytic hydrogen evolution. Over the past few years, intensive research has been focused on transition metal oxides such as ZnO, TiO_2, Fe_2O_3, *etc.*[13–15] However, little attention has been paid to rare earth oxides, which have been widely used in upconversion materials, high-quality phosphors, time-resolved fluorescence labels for biological detection, catalysts, and catalyst supports due to their outstanding optical and catalytic properties.[16–20] Recently, the optical, catalytic and electrical properties of CdS doped with rare earth elements have been studied,[1–23] but investigations of CdS/rare earth oxides heterostructures are still rarely reported. Thus it is highly desirable to investigate the properties of CdS/rare earth oxide heterostructures, especially for their photocatalytic activity.

To evaluate this issue, we examined a combination of CeO_2 and CdS for photocatalytic hydrogen generation because CeO_2 has a suitable band gap (3.2 eV). Moreover, CeO_2 has been recently used as a photoactive material in solar cells and a photocatalyst in the degradation of dye pollutants and hydrogen evolution.[24–28] In this communication, we first describe a facile one-pot electrochemical approach to fabricate monodisperse CeO_2/CdS heterostructured spheres and the investigation of their photocatalytic activity in hydrogen evolution from hydrogen generation. Well-dispersed and highly-crystalline CeO_2/CdS heterostructured spheres with diameters of about 500 nm were directly grown on FTO substrates *via* electrodeposition from aqueous solution. These CeO_2/CdS heterostructured spheres exhibit a high photocatalytic performance in hydrogen production from hydrogen generation. CeO_2/CdS heterostructured spheres were obtained *via* electrodeposition in an aqueous solution of 0.005 M $Ce(NO_3)_3{\cdot}6H_2O$ + 0.005 M $Cd(NO_3)_2{\cdot}4H_2O$ + 0.1 M CH_4N_2S with a current density of 0.6 mA cm^{-1} for 120 min. The reaction temperature was kept at 90 °C.

The crystal structures of the products were identified by X-ray diffraction (XRD), and a typical XRD pattern is shown in Fig. 1a. Most of the diffraction peaks can be assigned to the fluorite cubic structure of CeO_2 (JCPDF # 65-2975) with lattice constants a = 5.411 Å and the hexagonal structure of CdS (JCPDF # 41-1049) with lattice constants a = 4.14 Å and c = 6.72 Å. Compared to the weak diffraction peaks of the CeO_2 phase, the sharp diffraction peaks of the CdS phase suggest the product is largely made up of CdS and has the higher crystallinity of CdS. No peaks of impurities are detected besides SnO_2 peaks that originate from the substrates, which reveals the high purity of the as-synthesized products. SEM images in Fig. 1 and Fig. S1 (ESI†) clearly show that the products consist of a great deal of sphere-like CeO_2/CdS architectures. These spheres have an average diameter of about 500 nm and are dispersed on FTO substrates with good monodispersity. Besides, it should be

[a]*KLGHEI of Environment and Energy Chemistry, MOE Laboratory of Bioinorganic and Synthetic Chemistry, School of Chemistry and Chemical Engineering, Institute of Optoelectronic and Functional Composite Materials, Sun Yat-sen University, Guangzhou, 510275, P. R. China. E-mail: chedhx@mail.sysu.edu.cn; Fax: +86 20 84112245; Tel: +86 20 84110071*
[b]*School of Physics and Engineering, Sun Yat-Sen University, Guangzhou, 510275, P. R. China*

† Electronic supplementary information (ESI) available: Detailed experimental section, SEM image, EDX elemental line mapping images and XPS spectra of CeO_2/CdS heterostructured spheres. See DOI: 10.1039/c1ra00252j

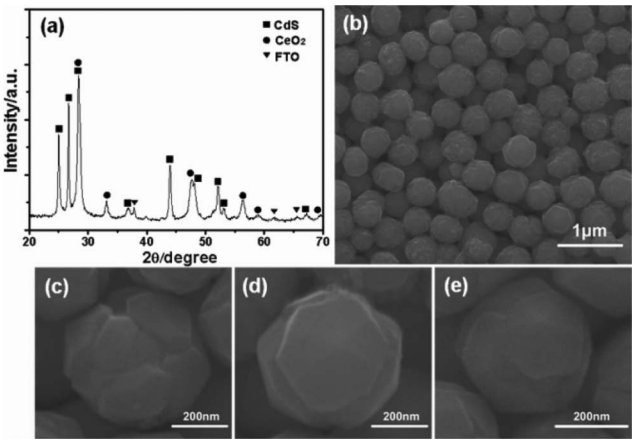

Fig. 1 (a) XRD pattern and (b–e) SEM images of as-synthesized CeO_2/CdS heterostructured spheres.

noted that the surface morphology of the spheres is coarse, and three representative morphologies of CeO_2/CdS heterostructured spheres are presented in Fig. 1c–e.

More-detailed structural information of the CeO_2/CdS heterostructured spheres was provided by transmission electron microscopy (TEM). Fig. 2a shows the TEM image of a typical CeO_2/CdS sphere with a diameter of 350 nm, showing the sphere is irregular. The inset in the upper right position of Fig. 2c is the selected area electron diffraction (SAED) pattern recorded from region b of Fig. 2a. The diffraction spots of hexagonal CdS are clearly observed and can be well indexed to (100), (101), (101) planes and/or their equivalent planes under the incident electron beam along the [010] direction. And these sharp diffraction spots reveal the single crystalline nature of CdS. In addition to those bright spots, there are two weak diffraction rings in this SAED pattern, which correspond to the (111) and (200) planes of the polycrystalline cubic CeO_2. The high-resolution TEM (HRTEM) image taken in region b of Fig. 2a (Fig. 2b) shows a distinct lattice fringe pattern, indicating the highly

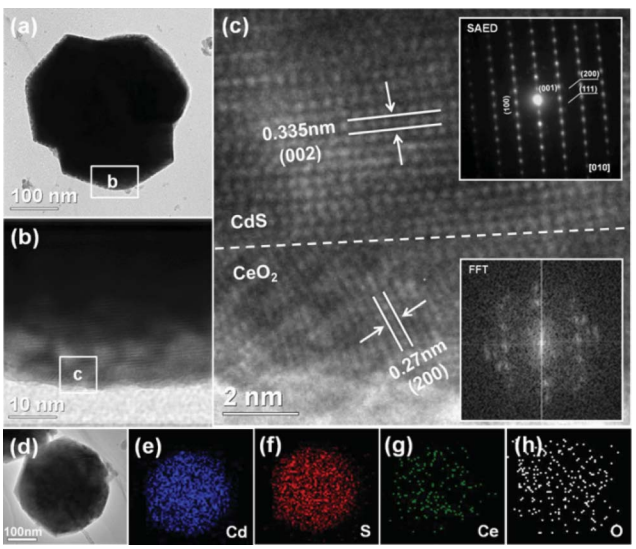

Fig. 2 (a, d) TEM and (b, c) HRTEM images of as-synthesized CeO_2/CdS heterostructured spheres. The insets in Fig. 2c are the corresponding SAED and FFT patterns. (e–h) EDX elemental mapping images of the Cd, S, Ce and O, respectively.

crystalline nature of the CeO_2/CdS heterostructured sphere. To better investigate the crystal structure of this heterostructured sphere, an enlarged HRTEM image and its corresponding fast Fourier transform (FFT) pattern are shown in Fig. 2c. The clear lattice fringe with a *d*-spacing of 0.335 nm belongs to the lattice fringe of the (100) plane of the hexagonal CdS, while the lattice fringe of 0.27 nm is assigned to the (200) plane of the cubic CeO_2. Hence, based on the results above, it is evident that the sphere is a heterostructure, which is made up of single crystalline CdS and polycrystalline CeO_2. To our knowledge, this is the first report of the one-pot synthesis of CeO_2/CdS heterostructured spheres. In order to further elucidate microscopic structure, TEM-EDX (energy dispersive X-ray) elemental full and line mapping techniques were applied to an individual sphere. The results are shown in Fig. 2d–h and Fig. S2.† It can be seen that Cd, S, Ce and O are uniformly distributed on the surface of the sphere. The content of CdS is far greater than that of CeO_2, and their atom ratio is about 3 : 1. X-Ray photoelectron spectroscopy (XPS) was also conducted to study the structure of the CeO_2/CdS spheres. According to the corresponding XPS spectra in Fig. S3,† these heterostructured spheres could be indexed to the chemical form of CdS and CeO_2, and the atom ratio of Cd and Ce is 19.36 : 6.35. The results are consistent with the XRD and EDS.

The one-pot formation process of CeO_2/CdS spheres is proposed as follows: the nitrate ions was first electro-reduced to form hydroxyl ions (OH^-) on the surface of the cathode *via* eqn (1) according to previous work.[29] The generated OH^- will react with Ce^{3+} to produce $Ce(OH)_3$. Since the $Ce(OH)_3$ is unstable it changes into CeO_2 immediately in the presence of the dissolved oxygen (eqn (2)). Meanwhile, $S{=}C(NH_2)_2$ is coordinated to cadmium through the sulfur atom. At high temperatures, the S=C bonds are broken by the attack of the strongly nucleophilic O atoms of H_2O molecules and release S^{2-} (eqn (3)). The applied electric field drives Cd^{2+} to migrate towards the surface of the cathode and will react with free S^{2-} ions to form CdS (eqn (4)).[30] In addition, it is easy to form CeO_2 and CdS due to the $K_{sp Ce(OH)_3} = 1.5 \times 10^{-20}$, $K_{sp Ce_2S_3} = 4.4 \times 10^{-20}$, $K_{sp CdS} = 8 \times 10^{-27}$, $K_{sp Cd(OH)_2} = 2.5 \times 10^{-14}$.[31] Finally, The produced CdS and CeO_2 will mix at molecular level, and they can uniformly enter into each crystal lattices, leading to the formation of CeO_2/CdS.

$$NO_3^- + H_2O + e \rightarrow NO_2^- + 2OH^- \quad (1)$$

$$4Ce^{3+} + 12OH^- + O_2 \rightarrow 4CeO_2 + 6H_2O \quad (2)$$

$$S{=}C(NH_2)_2 + H_2O \rightarrow O{=}C(NH_2)_2 + 2H^+ + S^{2-} \quad (3)$$

$$Cd^{2+} + S^{2-} \rightarrow CdS \quad (4)$$

Heterostructured CeO_2/CdS spheres were further used as a photocatalyst for hydrogen generation. Typically, 0.050 g of powder sample was dispersed in 100 mL aqueous solution containing 0.43 M Na_2S and 0.50 M Na_2SO_3 in a Pyrex reaction cell with continuous strong stirring. The light source was a 300 W Xe lamp (PLS-SXE-300UV, Beijing Changtuo) supplying full wavelength illumination. The amount of produced hydrogen was analyzed using on-line gas chromatography with a thermal conductivity (TCD) detector and a nitrogen carrier. For comparison, the same study was also examined using commercial CdS, CeO_2 and their mixture, and the results are shown in Fig. 3. It was observed that the hydrogen evolution rate of the CeO_2/CdS heterostructured spheres is about 782 μmol g^{-1} h^{-1}, which

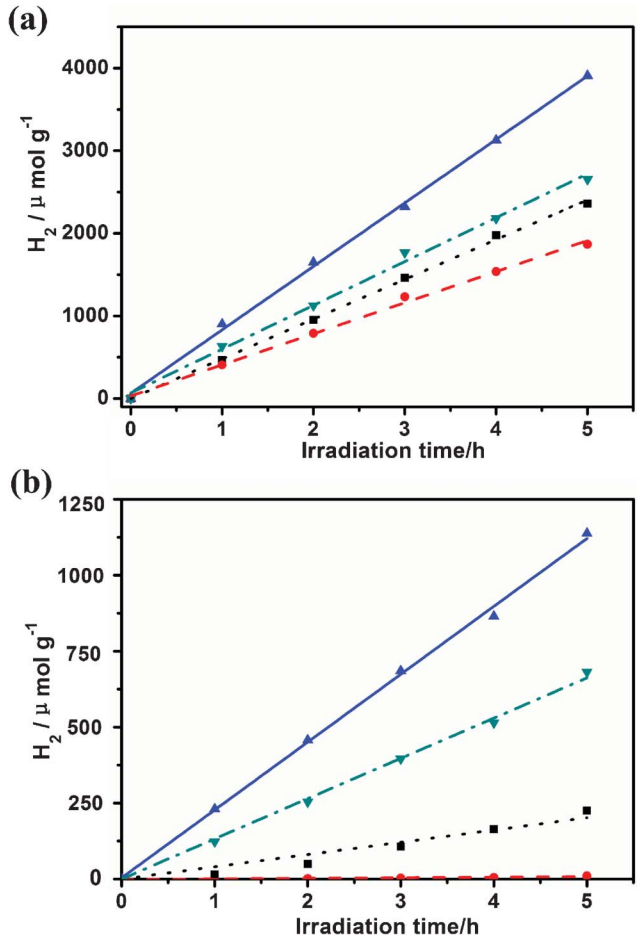

Fig. 3 Under (a) full wavelength and (b) visible light ($\lambda \geqslant 420$ nm) illumination in Na_2S–Na_2SO_3 (0.43 M : 0.5 M) mixture solution, hydrogen production rates of: commercial CdS (dotted line); commercial CeO_2 (dashed line); CeO_2/CdS spheres (solid line); CeO_2/CdS mixture (25 at% CeO_2 : 75 at% CdS, dash dot line).

is much higher than those of commercial CdS (487 μmol g^{-1} h^{-1}) and CeO_2 (384 μmol g^{-1} h^{-1}). Besides, it is noted that the photocatalytic activity of the CeO_2/CdS heterostructured spheres is also superior to that of the CeO_2/CdS mixture (25 at% CeO_2 : 75 at% CdS), indicating that the intimately contacted semiconductor system is more efficient. Similar results are observed under visible light irradiation (with a UV-cut-off filter $\lambda \geqslant 420$ nm), and the hydrogen evolution rate of the CeO_2/CdS heterostructured spheres reached 223 μmol g^{-1} h^{-1}, which is also much higher than those of commercial CdS (40 μmol g^{-1}) and CeO_2 (almost no hydrogen was detected), while the rate of the CeO_2/CdS mixture (25 at% CeO_2 : 75 at% CdS) is only 132 μmol g^{-1} h^{-1}.

On the basis of the above results, the enhancement of the photocatalytic hydrogen activity of the CeO_2/CdS heterostructured spheres is mainly due to their heterostructures, which formed a Z-scheme system in photocatalytic hydrogen generation. It is known that the conduction and valence bands of CeO_2 are formed by Ce 5d and O 2p orbitals, and the band-gap energy between them is about 6.0 eV. The unoccupied Ce 4f orbital with a narrow band (about 3.2 eV from O 2p to Ce 4f) locates between this band gap,[26,31] which potentially is close to that of the conduction band of TiO_2.[14] Thus, electron transfer from the conduction band of CdS to the conduction

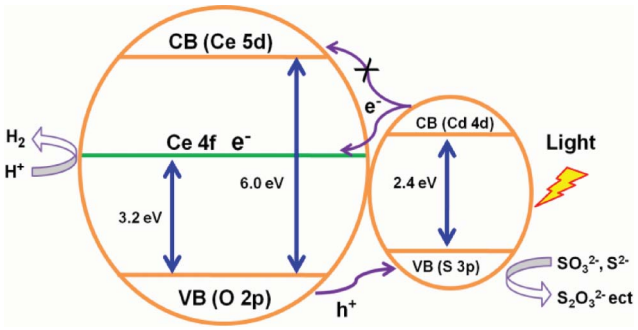

Fig. 4 The photocatalytic hydrogen evolution mechanism over the CeO_2/CdS heterostructured spheres.

band of CeO_2 is thermodynamically impossible, but from the conduction band of CdS to the 4f band of CeO_2 is thermodynamically possible, as illuminated in Fig. 4. In the CeO_2/CdS heterostructured spheres, the holes generated in the Ce 2p orbital can migrate to the Cd 3p orbital and react with SO_3^{2-} or S^{2-} in the heterostructured spheres' surface. At the same time, the photogenerated electrons in the Cd 4d orbital transfer to the Ce 4f orbital, react with H_2O and produce H_2. In a word, in the presence of CeO_2, the photogenerated holes and electrons can perfectly separate, which can enhance hydrogen generation.

In addition, CeO_2 could transfer the electron coming from photoexcited dye molecules quickly as a predominant electron-transfer medium, resulting in the enhancement of photocatalytic activity.[32] In our case, the photoexcited electrons will be first produced on the conduction band of CdS under light irradiation and inject into the Ce 4f orbital. Meanwhile, the photogenerated holes will flow from the valence band of CeO_2 (O 2p) to the valence band of CdS (S 3p). As a result, a Z-scheme system that can effectively reduce charge recombination is formed and hence improves the photocatalytic activity.

In summary, monodisperse CeO_2/CdS heterostructured spheres with high crystallinity have been successfully grown on FTO substrates by a simple and effective electrochemical method from aqueous solution. The photocatalytic hydrogen evolution experiments demonstrate that the CeO_2/CdS heterostructured spheres based on a Z-scheme mechanism have a superior performance to pure CdS, CeO_2 and their mixture. This finding suggests these CeO_2/CdS heterostructured spheres are a promising photocatalyst for hydrogen evolution. Moreover, the one-step growth of heterostructures on FTO substrates may further broaden their application as a photoactive material in fabricating optoelectronic devices.

Acknowledgements

We gratefully acknowledge financial support from the Natural Science Foundations of China (Grant No. 20873184, 90923008), the Natural Science Foundations of Guangdong Province (Grant No. 2008B010600040, 9251027501000002, 8151027501000095), and the Fundamental Research Funds for the Central Universities (101gzd13).

References

1 A. Kudo and Y. Miseki, *Chem. Soc. Rev.*, 2009, **38**, 253.
2 W. J. Youngblood, S.-H. A. Lee, K. Maeda and T. E. Mallouk, *Acc. Chem. Res.*, 2009, **42**, 1966.

3 R. Krol, Y.-Q. Liang and J. Schoonman, *J. Mater. Chem.*, 2008, **18**, 2311.
4 S. Chuangchote, J. Jitputti, T. Sagawa and S. Yoshikawa, *ACS Appl. Mater. Interfaces*, 2009, **1**, 1140.
5 R. M. Navarro, M. C. Alvarez-Galván, J. A. V. Mano, S. M. Al-Zahrani and J. L. G. Fierro, *Energy Environ. Sci.*, 2010, **3**, 1865.
6 N. Z. Bao, L. M. Shen, T. Takata and K. Domen, *Chem. Mater.*, 2008, **20**, 110.
7 I. Tsuji, H. Kato and A. Kudo, *Angew. Chem., Int. Ed.*, 2005, **44**, 3565.
8 S. Y. Ryu, W. Balcerski, T. K. Lee and M. R. Hoffmann, *J. Phys. Chem. C*, 2007, **111**, 18195.
9 D. Meissner, R. Memming and B. Kastening, *J. Phys. Chem.*, 1988, **92**, 3476.
10 X. Zong, G. P. Wu, H. J. Yan, G. J. Ma, J. Y. Shi, F. Y. Wen, L. Wang and C. Li, *J. Phys. Chem. C*, 2010, **114**, 1963.
11 X. W. Wang, G. Liu, Z. G Chen, F. Li, L. Z Wang, G. Q. Lu and H. M. Cheng, *Chem. Commun.*, 2009, 3452.
12 N. Strataki, M. Antoniadou, V. Dracopoulos and P. Lianos, *Catal. Today*, 2010, **151**, 53.
13 R. M. Navarro, F. Valle and J. L. G. Fierro, *Int. J. Hydrogen Energy*, 2008, **33**, 4265.
14 C. L. Li, J. Yuan, B. Y. Han, L. Jiang and W. F. Shangguan, *Int. J. Hydrogen Energy*, 2010, **35**, 7073.
15 H. McDaniel and M. Shim, *ACS Nano*, 2009, **3**, 434.
16 F. Zhang, Y. H. Deng, Y. F. Shi, R. Y. Zhang and D. Y. Zhao, *J. Mater. Chem.*, 2010, **20**, 3895.
17 M. Nyk, R. Kumar, T. Y. Ohulchanskyy, E. J. Bergey and P. N. Prasad, *Nano Lett.*, 2008, **8**, 3834.
18 F. Zhang, G. B. Braun, Y. F. Shi, Y. C. Zhang, X. H. Sun, N. O. Reich, D. Y. Zhao and G. Stucky, *J. Am. Chem. Soc.*, 2010, **132**, 2850.
19 B. M. E. Russbueldta and W. F. Hoelderich, *J. Catal.*, 2010, **271**, 290.
20 N. Perkas, G. Amirian, Z. Y. Zhong, J. Teo, Y. Gofer and A. Gedanken, *Catal. Lett.*, 2009, **130**, 455.
21 P. V. Jyothy, K. A. Amrutha, Jose Gijo and N. V. Unnikrishnan, *J. Fluoresc.*, 2009, **19**, 165.
22 J. A. Dávila-Pintle, R. Lozada-Morales, M. R. Palomino-Merino and J. A. Rivera-Márquez, *J. Appl. Phys.*, 2007, **101**, 013712.
23 K. Zhang, D. W. Jing, Q. Y. Chen and L. J. Guo, *Int. J. Hydrogen Energy*, 2010, **35**, 2048.
24 A. Corma, P. Atienzar, H. Garcia and J. Y. Chane-Ching, *Nat. Mater.*, 2004, **3**, 394.
25 M. Lira-Cantua and F. C. Krebs, *Sol. Energy Mater. Sol. Cells*, 2006, **90**, 2076.
26 H. Kadowaki, N. Saito, H. Nishiyama and Y. Inoue, *Chem. Lett.*, 2007, **36**, 440.
27 G. R. Bamwenda, K. Sayama and H. Arakawa, *Chem. Lett.*, 1999, 1047.
28 Y. S. Chaudhary, S. Panigrahi, S. Nayak, B. Satpati, S. Bhattacharjee and N. Kulkarni, *J. Mater. Chem.*, 2010, **20**, 2381.
29 L. Xu, Q. Chen and D. Xu, *J. Phys. Chem. C*, 2007, **111**, 11560.
30 X. B. He and L. Gao, *J. Phys. Chem. C*, 2009, **113**, 10981.
31 D. D. Koelling, A.M. Boring and J. H. Wood, *Solid State Commun.*, 1983, **47**, 227.
32 P. F. Ji, J. L Zhang, F. Chen and M. Anpo, *Appl. Catal., B*, 2009, **85**, 148.

